Carbon-Centered Radicals

DOI: 10.1002/ange.201300668

Formation of Trichlorosilyl-Substituted Carbon-Centered Stable Radicals through the Use of π-Accepting Carbenes**

Kartik Chandra Mondal, Herbert W. Roesky, A. Claudia Stückl, Fabian Ehret, Wolfgang Kaim,* Birger Dittrich,* Bholanath Maity, and Debasis Koley**

Dedicated to Professor Werner Uhl on the occasion of his 60th birthday

Carbon or silicon radicals with silyl substituents are important intermediates in organometallic and organic chemistry.[1] Already in 1970, Bassindale et al. had reported the persistent tris(trimethylsilyl)methyl radical,[2] $(Me_3Si)_3C^{\bullet}$, which has a lifetime of several days at 298 K. The groups of Ingold,[3] Apeloig,[4] Bravo-Zhivotovskii,[5] Lee,[6] Sekiguchi,[7] and others[4–6] have shown that the lifetime of the radicals largely depends on the steric bulk of the substituents. In 2002, Sekiguchi et al.[7] reported the first stable silicon-centered radical without any π conjugation. Several reports describe the preparation of this class of radicals. The most successful ones proceed through the photolytic or thermal cleavage of a Si–Si bond, and $R_3Si–SiHCl_2$ can be reacted with bulky reagents, such as $(t\mathrm{Bu})_2\mathrm{MeSiLi}$, according to the Apeloig–Sekiguchi method. Several radical species[8] of main-group elements, such as $PN^{\bullet+}$,[8b] $P_2^{\bullet+}$,[8c] phosphinyl radical cations,[8d] $HB^{\bullet+}$,[8e] and ketenes with biradical character,[8f] were also stabilized by cyclic alkyl(amino) carbenes (cAACs). We have observed that the chemical response of cAACs[8a] toward silylenes is very different from that of N-heterocyclic carbenes (NHCs). Recently, we have demonstrated that NHC→$SiCl_2$ **1** reacts with Me_2-cAAC in a redox reaction to form the biradical (Me_2-cAAC$^{\bullet}$)$_2SiCl_2$ **2** in a two-electron redox step.[8g] Consequently, we were curious to investigate the one-electron redox process. Therefore, we reacted cAAC→$SiCl_4$ **3** with KC_8 in an equimolar ratio in *n*-hexane to yield stable radicals **4**, of the general formula (cAAC$^{\bullet}$)–$SiCl_3$.

The highly reactive trichloromethane radical $CCl_3^{\bullet}$[9a] and its congener $SiCl_3^{\bullet}$[9b] are frequently generated by flash photolysis. These species are active radical intermediates in many photochemical transformations.[9a,b] Recently, the chemical reactivity of the TEMPO radical towards $SiCl_4$[9c] and metal ions[9d] was explored, and the catalytic[9d] and fashionable magnetic[9e,f] properties of these adducts were studied. Although handling and controlling the chemical behavior of radicals can be very difficult, the chemistry of radicals has always been captivating.[10,11]

To the best of our knowledge, stable radicals with the $SiCl_3$ group next to the radical center have not been reported so far. The carbene carbon atom of an NHC is bound to two both σ-withdrawing and π-donating nitrogen atoms. In a cAAC, one nitrogen atom of the NHC is replaced by a σ-donating quaternary carbon atom. Theoretical calculations showed that the HOMO–LUMO energy gap is smaller in cAACs. Thus, cAACs are both more nucleophilic and more electrophilic than NHCs.[12a] Recently, ^{31}P NMR analysis of a number of carbene–phenylphosphinidene adducts revealed that cAACs are better π acceptors than NHCs.[12b] These inherent differences may play a pivotal role in the replacement of an NHC by a cAAC and their behavior in a reaction. The NHC→$SiCl_4$ adduct was reduced to NHC→$SiCl_2$, (NHC→$SiCl)_2$, and NHC→Si=Si←NHC through the use of KC_8.[13] In detail, an equimolar mixture of cAAC→$SiCl_4$ **3** (1 mmol) and KC_8 (1 mmol) in *n*-hexane (85 mL) was initially reacted at −78 °C. The resulting suspension was slowly warmed to room temperature to obtain a clear colorless solution and an unreacted deposit of insoluble KC_8. Upon stirring for 24 h, the color of the solution changed to a clear light yellow with the black deposit of graphite; after filtration, the solution was concentrated to a volume of 2–3 mL to obtain fluorescent yellow plates/needles of the (cAAC$^{\bullet}$)-$SiCl_3$ radical **4**. Herein, we report the synthesis, structural correlation, DFT calculations, and EPR studies of the two carbon-centered radicals **4a** and **4b** (Scheme 1).

The syntheses of **3a** and **3b** are described in the Supporting Information. The melting points of compounds **3a**, **3b**, **4a**, and **4b** range from 105 °C to 118 °C. The color of compounds **4a** and **4b** is a fluorescent yellow, whereas **3a** and **3b** are colorless, as expected. Compounds **4a** and **4b** are soluble in toluene, benzene, and THF, whereas **3a** is only soluble in THF, and **3b** is only sparingly soluble in this solvent. Compounds **3a**, **3b**, **4a**, and **4b** are stable in inert

[*] Dr. K. C. Mondal, Prof. Dr. H. W. Roesky, Dr. A. C. Stückl
Institut für Anorganische Chemie, Universität Göttingen
Tammannstrasse 4, 37077 Göttingen (Germany)
E-mail: hroesky@gwdg.de
Dipl.-Chem. F. Ehret, Prof. Dr. W. Kaim
Universität Stuttgart, Institut für Anorganische Chemie
Pfaffenwaldring 55, 70569 Stuttgart (Germany)
E-mail: kaim@iac.uni-stuttgart.de
Priv.-Doz. Dr. B. Dittrich
Institut für Anorganische und Angewandte Chemie, Universität Hamburg, Martin-Luther-King-Platz 6, 20146 Hamburg (Germany)
E-mail: birger.dittrich@chemie.uni-hamburg.de
M. Sc. B. Maity, Dr. D. Koley
Department of Chemical Sciences, Indian Institute of Science Education and Research Kolkata
Mohanpur Campus, PO: BCKV Campus Main Office, Mohanpur—741252, Nadia, West Bengal (India)
E-mail: koley@iiserkol.ac.in

[**] H.W.R. thanks the Deutsche Forschungsgemeinschaft (RO 224/60-I) for financial support. B.M. is thankful to the CSIR for a research fellowship. D.K. acknowledges the IISER-Kolkata for a start-up grant and the SERB for a DST fast track fellowship (SR/FT/CS-72/2011).

Supporting information for this article is available on the WWW under http://dx.doi.org/10.1002/anie.201300668.

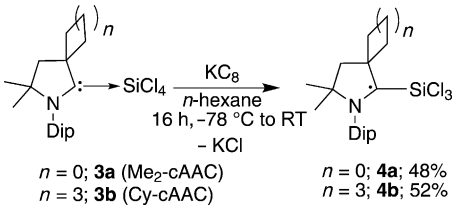

Scheme 1. Syntheses of compounds **4a** and **4b** from **3a** and **3b**, respectively through KC_8 reduction. Dip = 2,6-diisopropylphenyl.

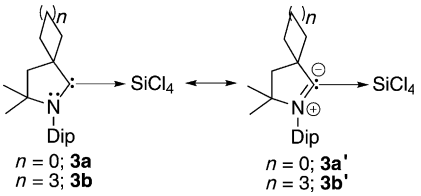

Scheme 2. Zwitterionic resonance structures **3a′** and **3b′** of the adducts **3a** and **3b**.

atmosphere for more than three months in both the solid state and in solution. Both the mono-radical compounds **4a** (m/z = 420.1 [M^+]) and **4b** (m/z = 462.1 [M^+]) were characterized by electron ionization mass spectrometry.

All compounds were characterized by single-crystal X-ray diffraction with the exception of **3b** because of its poor solubility (see the Supporting Information). The UV/Vis spectra of **4a** and **4b**, which were recorded in *n*-hexane, show a similar signature between 400 nm and 200 nm (see the Supporting Information). Compounds **4a** and **4b** exhibit absorption bands at 260, 300, and 335 nm, with a hump of low intensity at 405 nm (see the Supporting Information).

There are no absorption bands above 500 nm for **4a** and **4b**, whereas for the biradical (Me_2-cAAC$^{\bullet}$)$_2SiCl_2$ **2** and biradicaloid siladicarbene (Me_2cAAC)$_2$Si **5** absorptions were detected at higher values: 569 nm for **2**,[8g] and 569 nm and 611 nm for **5**.[10] The one-electron paramagnetic bulk radical properties of **4a** and **4b** were confirmed by magnetic susceptibility measurements (see the Supporting Information). The room-temperature value of χT is 0.37 $cm^3 K mol^{-1}$ for both **4a** and **4b**, which is in excellent agreement with the value expected for one unpaired electron. The χT versus T plots of **4a** and **4b** show that the χT values remain constant at 0.37 $cm^3 K mol^{-1}$ from room temperature to 25 K, below which they slightly decrease because of weak intermolecular antiferromagnetic interactions (see the packing diagrams in the Supporting Information).

The ^{29}Si and ^{13}C NMR spectra of **3a** exhibit resonances at −103.5 and 206.1 ppm, respectively. The corresponding ^{13}C resonance is shifted upfield compared with that of Me_2-cAAC (304.2 ppm), but shifted slightly downfield relative to that of the Me_2cAACH$^+$OTf$^-$ salt (192.2 ppm). The NHC→$SiCl_4$ adduct exhibits[12] a resonance in its ^{29}Si NMR spectrum at −108.9 ppm, which is close to that of **3a** at −103.5 ppm. Comparable resonances were not observed for compounds **4a** and **4b**, owing to their radical nature, whereas their ^{1}H NMR spectra showed broad signals.

X-ray single crystal diffraction was performed at 100 K. The adduct **3a** crystallizes both with and without THF as the lattice solvent. **3a** and **3a**·THF crystallize in the orthorhombic and monoclinic space groups $P2_12_12_1$ and $P2_1/c$, respectively. The crystal structure of **3a** reveals that the silicon atom adopts a distorted trigonal bipyramidal geometry and is surrounded by four chlorine atoms and the carbene carbon atom of Me_2-cAAC. The Si–C bond distances are 194.4(2) pm (**3a**) and 192.9(2) pm (**3a**·THF), which are close to the reported value of 192.8(2) pm for NHC→$SiCl_4$, thus suggesting a coordinate bond between the carbene carbon of Me_2-cAAC and $SiCl_4$. The Si–Cl bond lengths range from 205.81(9) pm to 219.64(10) pm for **3a** and from 206.59(10) pm to 221.30(10) pm for **3a**·THF. The C(carbene)–N bond lengths are 130.40(2) pm (**3a**) and 130.6(3) pm (**3a**·THF), which are close to those values (ca. 131.5 pm) found for the analogous free carbene or Pd–carbene adducts,[8a] but slightly shorter than that of (Me_2-cAAC$^{\bullet}$)$_2SiCl_2$ **2** (139.94(19) pm).[8g]

Moreover, the N-C(carbene)-C angle is slightly wider than that of **2** (see the Supporting Information). Thus, the lone pair of electrons on the nitrogen atom is more delocalized on the vacant *p*-orbital of the carbene carbon of **3a**/**3a**·THF. However, experimental data and ab initio calculations have established that the C=N bond distances of alkyl-substituted imines are ca. 130 pm.[14] Thus **3a**/**3a**·THF and **3b** can be regarded as zwitterionic adducts (**3a′** and **3b′**), as shown in Scheme 2. The salt Cy-cAACH$^+$OTf$^-$ **6** (Cy = cyclohexyl, OTf = trifluoromethanesulfonate) was also investigated by single-crystal X-ray diffraction to further characterize the flexible nature of the C=N bond (128.03(15)/128.58(15) pm; see the Supporting Information).

Compound **4a** crystallizes in the orthorhombic space group *Pbca*. Interestingly, **4b** shows polymorphism and crystallizes in two different space groups, although both solid state forms were formed from the *n*-hexane solutions. Polymorph I of **4b**, which crystallized at 0 °C, appeared as yellow needles after one week. Polymorph II of **4b** crystallized as yellow plates from a concentrated solution at room temperature within one to two hours. Polymorphs I and II crystallize in the monoclinic ($P2_1/n$) and triclinic ($P\bar{1}$) space groups, respectively. According to Ostwald's rule of stages, polymorph II of **4b** is less stable because it crystallizes first. Thus, the monoclinic form is the most stable polymorph of **4b**.

Both **4a** and **4b** contain one tetra-coordinate silicon atom, which is bound to three chlorine atoms and one carbene carbon atom. The silicon atom adopts a distorted tetrahedral geometry (Figure 1). The Si–C1 bond distances are in the expected range of 203.96(4)–206.48(4) pm (**4a**) and 203.45(3)–205.91(3) pm (**4b**). The high precision (low standard uncertainties) of these bond distances were achieved by "invariom" aspherical-atom refinements.[15] Similar bond distances are found in **2**.[8g] The Si–C(carbene) distances in **4a** and **4b** are 181.52(12) pm and 181.93(8) pm, respectively. A similar Si–C bond length was reported for the biradical *para*-3,6-bis[bis(di-*tert*-butylmethylsilyl)silylidene]-cyclohexa-1,4-diene (181.74(14) pm), which has a closed-shell partially quinoidal form with some contributions from the singlet bis(silyl radical) character.[11a] The Si–C(carbene) bond lengths in **4a** and **4b** are even shorter than those of the covalent Si–C bond of **2** (184.55(16) pm and 184.82(17) pm).[8g] However, the Si–C distances in **4a** and

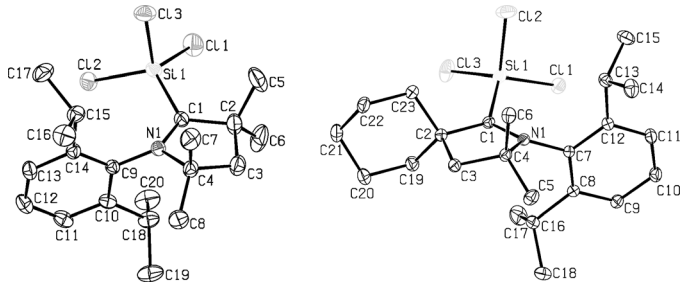

Figure 1. ORTEP view of the molecular structures of compound **4a** (left) and polymorph II of **4b** (right). Selected bond lengths [pm] and angles [°] (calculated values at the M05-2X/SVP level of theory are given in square brackets): **4a**/**4b**; C1–Si1 181.52(12)[*182.07*]/ 181.93(8)[*182.26*], C1–N1 137.79(14)[*138.04*]/138.27(10)[*138.08*], Si1–Cl1 203.96(4)[*206.86*]/203.45(5)[*206.41*], Si1–Cl2 204.12(4)[*206.31*]/ 205.91(3)[*208.66*], Si1–Cl3 206.46(4)[*208.64*]/204.05(3)[*206.96*]; C1-Si1-Cl1 111.64(5) [*111.29*]/114.34(3)[*114.98*], C1-Si1-Cl2 116.21(4)[*115.36*]/ 113.31(3) [*112.06*], C1-Si1-Cl3 112.23(5)[*112.15*]/112.37(3)[*112.26*], Cl1-Si1-Cl2 106.37(2)[*106.19*]/104.659(13)[*105.64*], Cl1-Si1-Cl3 105.34(2) [*105.60*]/105.838(13)[*105.78*], Cl2-Si1-Cl3 104.19(2)[*105.54*]/ 105.528(13)[*105.35*], N1-C1-C2 109.99(11)[*110.52*]/110.55(6)[*110.71*].

4b are longer than Si=C double bonds (170.2–177.5 pm).[16] The C(carbene)–N bond lengths are 137.79(14) pm (**4a**) and 138.27(10) pm (**4b**), which are close to those (139.94(19) pm) obtained for the biradical (Me_2-cAAC•)$_2SiCl_2$ (**2**).[8g]

The X-band EPR spectra of (Me_2-cAAC•)-$SiCl_3$ (**4a**) and (Cy-cAAC•)-$SiCl_3$ (**4b**) (in a C_6D_6 solution) were recorded at room temperature. The spectrum of **4b** is shown (Figure 2, top). The spectra of **4a** and **4b** are very similar, with partially resolved hyperfine lines centered at $g = 2.00544$ (**4a**) and 2.00529 (**4b**).

In agreement with DFT calculations, including spin-density determination (Figure 2; see also the Supporting Information, Figures S17–S19) and computed hyperfine coupling constants (Tables S11 and S12), the simulation of the best-resolved experimental EPR spectrum (Figure 2) reveals a ^{14}N coupling constant ($I = 1$) of 6.4 Gauss, and smaller couplings of about 3.4 Gauss (1 Cl) and 2.7 G (2 Cl), with three Cl atoms ($I = 3/2$, nat. abundance of ^{35}Cl: 75.77 %, ^{37}Cl: 24.23 %; gyromagnetic ratio = 1.20). The relatively intense outermost lines suggest the non-equivalence of the chlorine couplings and thus a (partially) hindered rotation of the $SiCl_3$ group. In Figure 2, we have included the best simulation with non-equivalent Cl atoms (1 Cl 3.4 Gauss, 2 Cl 2.7 Gauss, each for ^{35}Cl) without the inclusion of any ^1H hyperfine splitting constants (hfsc). Hyperfine coupling from protons on the substituents are negligible with respect to line width (< 1.5 Gauss) because of their distance from the carbon radical center, whereas the coupling from ^{13}C ($I = 1/2$) and ^{29}Si ($I = 1/2$) is not observed owing to the low natural abundance (< 5 %) of these isotopes.

DFT optimization of **4a** and **4b** was performed for the doublet states at the UM05-2X/SVP level of theory (see the Supporting Information). The optimized structures show strong resemblance to the X-ray crystal structures, as seen from the alignments and superpositions of the respective structures. The calculations (Figure 2, bottom) reveal that the unpaired electron is primarily located on the carbene carbon (ca. 52 %), with a comparatively lower contribution from the

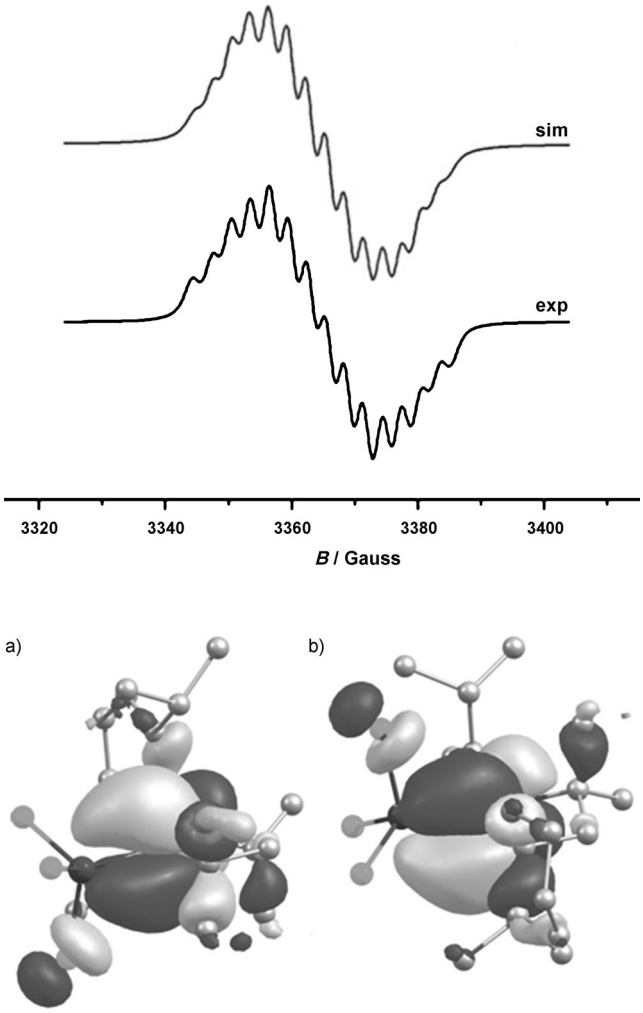

Figure 2. Experimental and simulated X-band EPR spectra (top) of a solution of **4b** in C_6D_6 at 298 K ($\nu_{\mu W} = 9.4387$ GHz, $B_{mod} = 0.5$ G at 100 kHz); the complete set of the simulation parameters is provided in the Supporting Information. The KS-SOMO (bottom) of a) **4a** and b) **4b** at the UM05-2X/TZVP//UM05-2X/SVP level of theory.

N1 atom (23 %) present in the cAAC fragment. The remaining 25 % of the electron density is scattered over the Dip and cAAC units and one of the Cl atoms. Calculations also revealed a slight charge transfer of 0.405 *e* and 0.358 *e*, respectively, from the $SiCl_3$ unit to the cAAC fragment for **4a** and **4b**. This may be due to the presence of the more electronegative carbene carbon atom, whose electron-withdrawing capability is further increased by the neighboring N1 atom. The Mulliken spin–density plots and values for **4a** and **4b** at the UM05-2X/TZVP//UM05-2X/SVP level are shown in Figures S17 and S18. The calculated spin densities show that the unpaired electron is located on the carbene carbon atom for both **4a** and **4b**, with a minor amount on the neighboring N1 atom. Furthermore, the spin density at silicon is negligible, which is in accordance with the previous calculations on the (Me_2-cAAC•)$_2SiCl_2$ system.[8g]

In conclusion, we have systematically studied the chemical behavior of a cAAC carbene toward $SiCl_4$. We found that the cAAC carbene forms zwitterionic adducts cAAC→$SiCl_4$, as exemplified with **3a′** and **3b′** (Scheme 2), which we

concluded from X-ray diffraction analysis. The zwitterionic nature of these adducts is responsible for their poor solubility in nonpolar solvents. The adducts are converted into stable and isolable trichlorosilylcarbene radicals (cAAC•)–$SiCl_3$ **4a** and **4b** through KC_8 reduction. As a consequence, the bond between the silicon atom and the carbene carbon atom dramatically changes its nature from a coordinate bond in **3a** and **3b** to a covalent bond in **4a** and **4b**. Such behavior of cAACs has no precedence in NHCs. Thus, the adjustable bonding nature between the electron-donating cAAC and the acceptor opens up another route toward the generation of a radical center just next to an acceptor with the general formula $(cAAC^{\bullet})_m$-EX_n [(E = metal or metalloid; $n = 0$, 1, 2, 3, $m = 1$, 2, 3, etc.; X = halide, R, etc.), which will find important chemical applications in the future. Moreover, compound **4b** was characterized in two polymorphic solid state forms. Compounds **4a** and **4b** are mono radicals, as confirmed by bulk magnetic susceptibility measurements in the solid state, EPR spectroscopy, and DFT calculations.

Experimental Section

(Me_2-cAAC•)-$SiCl_3$ **4a**: The solvent, *n*-hexane (85 mL), was added to a mixture of Me_2-cAAC→$SiCl_4$ **3a** 1 mmol) and KC_8 (1 mmol) at −78 °C. The suspension was slowly warmed to room temperature to give a clear colorless solution and unreacted starting material. Upon stirring for 24 h, the color of the solution changed to a clear light yellow, and the black solid (graphite) was separated by filtration. The *n*-hexane solution was reduced to a volume of 1–2 mL, and stored at 0 °C in a refrigerator to form fluorescent yellow plates of **4a** in 48 % yield. Melting range 114–116 °C. UV/Vis absorption bands at 215, 262, 300, 337, and 405 (weak) nm.

(Cy-cAAC•)-$SiCl_3$ **4b**: A similar procedure to that for **4a** was followed, but Cy-cAAC→$SiCl_4$ **3b** (1 mmol) was used instead of Me_2-cAAC→$SiCl_4$ **3a**. The volume of the *n*-hexane solution was reduced to 2–3 mL, and the solution was stored at room temperature to form yellow plates of **4b** (polymorph II); however, storing the solution at 0 °C in a refrigerator yielded long yellow needles of **4b** (polymorph I). The yield was 52 % for polymorph II. Melting range 115–118 °C. UV/Vis absorption bands at 215, 263, 304, 337, and 405 (weak) nm.

(Me_2-cAAC•)-$SiCl_3$ **4a** (Me_2-cAAC = :C(CH_2)(CMe_2)$_2$N-2,6-*i*$Pr_2C_6H_3$): $M = 419.90\ g\,mol^{-1}$, orthorhombic, space group *Pbca*, $a = 1613.03(4)$ pm, $b = 1616.69(4)$ pm, $c = 1732.81(4)$ pm, $\alpha = \beta = \gamma = 90.0°$, $V = 4.51877(19)\ nm^3$, $Z = 8$, μ(Mo-K$_\alpha$) = 4.19 mm^{-1}, $T = 100(2)$ K, 57818 reflections measured, 4402 unique reflections, $R_{int} = 0.0380$, 257 parameters refined, $R1$ (all data) = 0.037, $R1$ [$I > 2\sigma(I)$] = 0.0250, $wR2$ (all data) = 0.024, $wR2$ [$I > 2\sigma(I)$] = 0.024, GOF = 2.81, largest diff. peak and hole 0.353×10^3 and $-0.193 \times 10^3\ e\,nm^{-3}$.

Polymorph II of (Cy-cAAC•)-$SiCl_3$ **4b** (Cy-cAAC = :C(CH_2)-(CMe_2)(C_5H_{10})N-2,6-*i*$Pr_2C_6H_3$): $M = 459.96\ g\,mol^{-1}$, triclinic, space group $P\bar{1}$, $a = 852.90(2)$ pm, $b = 908.51(2)$ pm, $c = 1621.98(4)$ pm, $\alpha = 77.3711(10)°$, $\beta = 79.6798(11)°$, $\gamma = 84.3915(12)°$, $V = 1.20433(5)\ nm^3$, $Z = 2$, μ(Mo-K$_\alpha$) = 3.98 mm^{-1}, $T = 100(2)$ K, 23763 reflections measured, 4277 unique reflections, $R_{int} = 0.022$, 288 parameters refined, $R1$ (all data) = 0.0200, $R1$ [$I > 2\sigma(I)$] = 0.0170, $wR2$ (all data) = 0.022, $wR2$ [$I > 2\sigma(I)$] = 0.022, GOF = 2.94, largest diff. peak and hole 0.36×10^3 and $-0.177 \times 10^3\ e\,nm^{-3}$.

Received: January 25, 2013
Revised: July 24, 2013
Published online: September 13, 2013

Keywords: carbenes · density functional calculations · EPR spectroscopy · radicals · radical-chlorine interactions

[1] a) D. Griller, K. U. Ingold, *Acc. Chem. Res.* **1976**, *9*, 13–19; b) R. G. Hicks, *Org. Biomol. Chem.* **2007**, *5*, 1321–1338.
[2] A. R. Bassindale, A. J. Bowles, M. A. Cook, C. Eaborn, A. Hudson, R. A. Jackson, A. E. Jukes, *Chem. Commun.* **1970**, 559–559.
[3] See reference [1a] and references therein.
[4] G. Molev, B. Turmanskii, D. Sheberla, M. Botoshansky, D. Bravo-Zhivotovskii, Y. Apeloig, *J. Am. Chem. Soc.* **2009**, *131*, 11698–11700.
[5] D. Sheberla, B. Tumanskii, D. Bravo-Zhivotovskii, G. Molev, V. Molev, V. Y. Lee, K. Takanashi, A. Sekiguchi, Y. Apeloig, *Organometallics* **2010**, *29*, 5596–5606.
[6] V. Y. Lee, A. Sekiguchi, *Acc. Chem. Res.* **2007**, *40*, 410–419, and references therein.
[7] A. Sekiguchi, T. Fukawa, M. Nakamoto, V. Y. Lee, M. Ichinohe, *J. Am. Chem. Soc.* **2002**, *124*, 9865–9869.
[8] a) V. Lavallo, Y. Canac, C. Präsang, B. Donnadieu, G. Bertrand, *Angew. Chem.* **2005**, *117*, 5851–5855; *Angew. Chem. Int. Ed.* **2005**, *44*, 5705–5709; b) R. Kinjo, B. Donnadieu, G. Bertrand, *Angew. Chem.* **2010**, *122*, 6066–6069; *Angew. Chem. Int. Ed.* **2010**, *49*, 5930–5933; c) O. Back, B. Donnadieu, P. Parameswaran, G. Frenking, G. Bertrand, *Nat. Chem.* **2010**, *2*, 369–373; d) O. Back, M. A. Celik, G. Frenking, M. Melaimi, B. Donnadieu, G. Bertrand, *J. Am. Chem. Soc.* **2010**, *132*, 10262–10263; e) R. Kinjo, B. Donnadieu, M. A. Celik, G. Frenking, G. Bertrand, *Science* **2011**, *333*, 610–613; f) V. Lavallo, Y. Canac, B. Donnadieu, W. W. Schoeller, G. Bertrand, *Angew. Chem.* **2006**, *118*, 3568–3571; *Angew. Chem. Int. Ed.* **2006**, *45*, 3488–3491; g) K. C. Mondal, H. W. Roesky, M. C. Schwarzer, G. Frenking, I. Tkach, H. Wolf, D. Kratzert, R. Herbst-Irmer, B. Niepötter, D. Stalke, *Angew. Chem.* **2013**, *125*, 1845–1850; *Angew. Chem. Int. Ed.* **2013**, *52*, 1801–1805.
[9] a) F. Danis, F. Caralp, B. Veyret, H. Loirat, R. Lesclaux, *Int. J. Chem. Kinet.* **1989**, *21*, 715–727; b) J. D. DeSain, L. E. Jusinski, C. A. Caatjes, *Phys. Chem. Chem. Phys.* **2006**, *8*, 2240–2248; c) S. Stefan, F. Belaj, T. Mald, R. Pietschnig, *Eur. J. Inorg. Chem.* **2010**, 289–297; d) J. J. Scepaniak, A. M. Wright, R. A. Lewis, G. Wu, T. W. Hayton, *J. Am. Chem. Soc.* **2012**, *134*, 19350–19353; e) A. Caneschi, D. Gatteschi, N. Lalioti, C. Sangregorio, R. Sessoli, G. Venturi, A. Vindigni, A. Rettori, M. G. Pini, M. A. Novak, *Angew. Chem.* **2001**, *113*, 1810–1813; *Angew. Chem. Int. Ed.* **2001**, *40*, 1760–1763.
[10] K. C. Mondal, H. W. Roesky, M. C. Schwarzer, G. Frenking, B. Niepötter, H. Wolf, R. Herbst-Irmer, D. Stalke, *Angew. Chem.* **2013**, *125*, 3036–3040; *Angew. Chem. Int. Ed.* **2013**, *52*, 2963–2967.
[11] a) T. Nozawa, M. Nagata, M. Ichinohe, A. Sekiguchi, *J. Am. Chem. Soc.* **2011**, *133*, 5773–5775; b) H. Tanaka, M. Ichinohe, A. Sekiguchi, *J. Am. Chem. Soc.* **2012**, *134*, 5540–5543.
[12] a) D. Martin, M. Soleilhavoup, G. Bertrand, *Chem. Sci.* **2011**, *2*, 389–399; b) O. Back, M. Henry-Ellinger, C. D. Martin, D. Martin, G. Bertrand, *Angew. Chem.* **2013**, *125*, 3011–3015; *Angew. Chem. Int. Ed.* **2013**, *52*, 2939–2943.
[13] a) Y. Wang, Y. Xie, P. Wei, R. B. King, H. F. Schaefer III, P. v. R. Schleyer, G. H. Robinson, *Science* **2008**, *321*, 1069–1071; b) R. S. Ghadwal, H. W. Roesky, S. Merkel, J. Henn, D. Stalke, *Angew. Chem.* **2009**, *121*, 5793–5796; *Angew. Chem. Int. Ed.* **2009**, *48*, 5683–5686.
[14] R. Macaulay, L. A. Burnelle, C. Sandorfy, *Theor. Chim. Acta* **1973**, *29*, 1–7.
[15] B. Dittrich, C. B. Hübschle, K. Pröpper, F. Dietrich, T. Stolper, J. J. Holstein, *Acta Cryst.* **2013**, *B69*, 91–104.
[16] V. Y. Lee, A. Sekiguchi, *Organometallic Compounds of Low-Coordinate Si, Ge, Sn and Pb: From Phantom Species to Stable Compounds*, Wiley, Chichester, **2010**, chap. 5, p. 1682.

